JCTC Journal of Chemical Theory and Computation

Article

pubs.acs.org/JCTC

Atomistic Simulations of the ZnO(1$\bar{2}$10)/Water Interface: A Comparison between First-Principles, Tight-Binding, and Empirical Methods

Svea große Holthaus,[†] Susan Köppen,[†] Thomas Frauenheim,[†] and Lucio Colombi Ciacchi*[,†,‡]

[†]Bremen Centre for Computational Materials Science, University of Bremen, Germany

[‡]Fraunhofer Institute for Manufacturing Technology and Advanced Materials IFAM, Bremen, Germany

ABSTRACT: We investigate the adsorption behavior of water over the zinc oxide (1$\bar{2}$10) surface starting from single molecules up to bulk liquid by means of atomistic molecular dynamics simulations. We compare results obtained with density-functional theory, density-functional tight binding, and a recently developed reactive force field. The methods perform comparably up to the level of a single monolayer of adsorbed water, predicting only small differences in adsorption energies and, as a consequence, adsorption geometries. These lie within the error bars of typical quantum mechanical calculations performed with different exchange-correlation functionals. However, the discrepancies among the methods have a dramatic effect on the dissociation equilibria and the structuring of liquid water layers in contact with the surface. Especially the different treatment of electrostatic interactions via self-consistent atomic point charges appears to heavily influence the simulation outcomes. Critical comparisons with experimental studies and possibly ad hoc reparametrizations of the semiempirical functionals may thus be necessary to study phenomena such as dissolution or biomolecular adsorption at ZnO surfaces within statistically relevant time and size scales.

1. INTRODUCTION

Nanostructured zinc oxide is used in numerous applications such as in dye-sensitized solar cells,[1] gas and moisture sensors,[2,3] or catalysts, for instance, for ozonation reactions.[4] Over the years, several methods have been introduced to fabricate ZnO nanowires, nanorods, or nanoparticles.[5−7] With decreasing volume-to-surface ratio, a precise characterization of the surface structure and reactivity becomes of peculiar interest. In particular, the different surface energies of different crystallographic planes determine the shape and growth direction of ZnO nanostructures.

The predominant crystal structure of ZnO is wurtzite, as early reported by Hoppe,[8] with lattice constant values of $a = b = 3.250$ Å and a c/a ratio of 1.602. The surface of zinc oxide nanostructures under atmospheric conditions is composed of 80% by the two nonpolar surfaces (10$\bar{1}$0) and (1$\bar{2}$10), and of 20% by the two polar surfaces (0001) and (000$\bar{1}$).[9] Zhang et al.[10] reported surface enthalphies for various anhydrous ZnO nanostructure surfaces ranging from 2.55 to 7.28 J/m^2, without a clear assignment of the different values to specific crystallographic directions. More precise estimates of surface structure and energies are achieved by means of atomistic simulations, which have been performed for ZnO at different levels of precision.[11−13] Theoretical works have revealed that the terminal Zn−O dimers of the two nonpolar surfaces relax with a tilt angle between 7° and 10° with respect to the surface plane, accounting for the composite ionic and covalent characteristics of the surface bonds. For the (1$\bar{2}$10) surface, the surface energy values computed by Meyer et al.[11] with Density Functional Theory (DFT) lie between 1.25 and 0.85 J/m^2 depending on the used exchange correlation (xc) functional (LDA or GGA, respectively). Similar values were obtained also by Moreira et al.[12] using the GGA PBE xc functional (0.74 J/m^2), and by Raymand et al.[14] using the hybrid B3LYP functional (1.39 J/m^2). On the basis of DFT calculations, a reactive force field (ReaxFF) for ZnO surfaces has been recently parametrized, which gives a surface energy of 1.45 J/m^2 for the (1$\bar{2}$10) plane.[14]

Because of the numerous applications of zinc oxide under humid or liquid conditions, the ZnO/water interface has become an increasingly important field of research. The interaction of single water molecules with the ZnO(10$\bar{1}$0) surface has been extensively investigated with DFT by Meyer et al.,[15,16] identifying a surface pattern with (2 × 1) periodicity at the water coverage of 1 monolayer (ML), in agreement with experimental observations. While at lower coverages a molecular adsorption mode is preferred, the formation of a strongly bound hydrogen-bonding network promotes the dissociation of every second water molecule in the ML structure. The occurrence of an equilibrium between molecularly and dissociatively adsorbed water at 1 ML coverage on the (10$\bar{1}$0) surface was also predicted by Raymand et al.[14] using MD simulations within the ReaxFF approach. With this formalism, the same authors observed an increased number of hydroxyl groups formed upon dissociative water adsorption in the case of stepped surfaces, especially when in contact with bulk liquid water.[17] Considering nonstoichiometric models of the two nonpolar surfaces under varying external conditions, Cooke et al.[18] proposed that, in contrast to the (10$\bar{1}$0) surface, a fully dissociated monolayer with (1 × 1) periodicity should be the favorable adsorption mode on the (1$\bar{2}$10) surface. This finding is in agreement with ReaxFF results for the same surface,[14] although the very small differences in energy (0.06 eV) between the hydrated and hydroxylated structures suggest that both adsorption modes could be present, especially for

Received: August 13, 2012
Published: October 10, 2012

   dx.doi.org/10.1021/ct3007106 | J. Chem. Theory Comput. 2012, 8, 4517−4526

larger surface areas.[18] A study of the different ZnO bond characteristics between the $(10\bar{1}0)$ surface and the adsorbed water revealed that it is possible to distinguish between dissociatively and molecular adsorbed water molecules by looking at the projected density of states.[19]

Most of the studies reviewed above are limited to small surface unit cells and low water coverages, as a consequence of the high computational cost associated with dynamical investigations of solid/liquid interfaces at the DFT level. However, reaching larger system sizes is fundamental for a predictive modeling of the behavior of ZnO nanostructures in complex environments. For instance, investigations of the toxic action of ZnO nanoparticles in single cells or animals seem to suggest a direct linking between particle dissolution kinetics and toxicity.[20] A theoretical understanding of such phenomena, which involve the interface between ZnO particle surfaces (decorated with a large number of steps, kinks, and other defects) and physiological solutions (containing dissolved ions, small organic molecules, and biological macromolecules), must necessarily rely on approximate simulation methods. Among these, accurate tight-binding schemes such as DFTB[21] or carefully parametrized reactive force fields[13] appear to be very promising for simulations where chemical interactions such as water dissociation, proton transfer reactions, or dissolution events cannot be neglected.

In this work, we perform a comparative study of full DFT, semiempirical DFTB, and empirical ReaxFF methods applied to the interface between the ZnO$(1\bar{2}10)$ surface and liquid water. We present a step-by-step investigation of this interface starting from the adsorption of single water molecules, going through the formation of a monolayer, up to bulk liquid water in contact with the surface. The structures, energetic stabilities, and electronic structure features of different adsorption configurations at increasing coverage will be analyzed, highlighting the differences between the three simulation methods. Particular attention will be paid to the dynamical evolution of the hydration layers in Molecular Dynamics (MD) simulations of the ZnO/water interface. Our aim is to provide a comprehensive reference study of the performance of both DFTB and ReaxFF, as a basis for future studies focusing on more complex processes such as dissolution and protein adsorption on ZnO nanoparticle surfaces.

2. METHODS

2.1. Calculation Protocols. Our DFT calculations are performed using the PBE GGA xc functional, ultrasoft pseudopotentials,[22] and plane-wave expansions until a cutoff value of 30 Ry (300 Ry) for the electronic wave functions (charge density), similarly as in previous studies concerning ZnO.[11] No corrections to the standard GGA formalism are necessary to reliably reproduce the basic physical properties of nonpolar ZnO surfaces, as shown by Calzolari et al.[19] The PWscf code[23] is used for all static calculations with geometry optimization, integrating the Brillouin zone at the Γ point only, except for the projected density of states (PDOS) analysis, in which a denser $(4 \times 4 \times 1)$ k-point grid is used. All structures are relaxed until forces are below a threshold of 10^{-5} eV/Å. Molecular dynamics simulations at room temperature (300 K) are performed with the CPMD code[24] at the Γ point, using a time step of 5 au and a fictitious electronic mass of 300 au. All systems are heated using a Nosé–Hoover thermostat applying a previously employed heating procedure.[25]

The DFTB calculations are performed with the DFTB+ code,[26] using the tight-binding parameter set *znorg* introduced in ref 12. The geometry optimizations at the DFTB level are performed using the conjugate gradient method on a $(2 \times 2 \times 2)$ Monkhorst–Pack grid for the k-point sampling, using a force error tolerance of 10^{-6} eV/Å. In the MD simulations, we include only the Γ point and apply a Nosé–Hoover thermostat with an integration time step of 1 fs. The ReaxFF calculations are performed with the LAMMPS code,[27] using the potential parametrization introduced by Raymand et al.[13] We employ the conjugate gradient method with a tolerance of 10^{-6} eV/Å for the geometry optimizations, and the Nosé–Hoover thermostat with an integration time step of 0.25 fs for the MD simulations.

2.2. Test Calculations. With our DFT setup, the optimized lattice parameters of the ZnO wurtzite structure are $a = b = 3.288$ Å, $c = 5.302$ Å, which are in good agreement with the experimental values[8] and previous DFT-PBE results (Table 1).

Table 1. Lattice Constants of Bulk Wurtzite ZnO (a and c) and Surface Energy of the $(1\bar{2}10)$ Crystal Facet (γ) Calculated Using DFT, DFTB, and ReaxFF

	a [Å]	c [Å]	γ [J/m^2]
DFT	3.29	5.30	0.84
DFTB[a]	3.28	5.25	0.73
ReaxFF[b]	3.29	5.30	1.45
exp.[c]	3.25	5.21	

[a]Reference 12. [b]Reference 13. [c]Reference 8.

The DTFB and ReaxFF approaches are also able to reproduce well the experimental ZnO lattice constants, as reported in refs 12 and 13, respectively, and summarized here in Table 1. Given the negligibly small differences in the lattice constants obtained with the three methods, in this work we use, for all calculations, the ones obtained by DFT. As an additional validation test of the interaction between ZnO surfaces and water, we have calculated the adsorption energies of a single water molecule on nine adsorption sites of the $(10\bar{1}0)$ surface, as thoroughly investigated by Meyer et al. (see Figure 1 in ref 16). In all nine cases, our obtained adsorption energy values matched the ones reported by Meyer et al., indicating that our simulation setup is

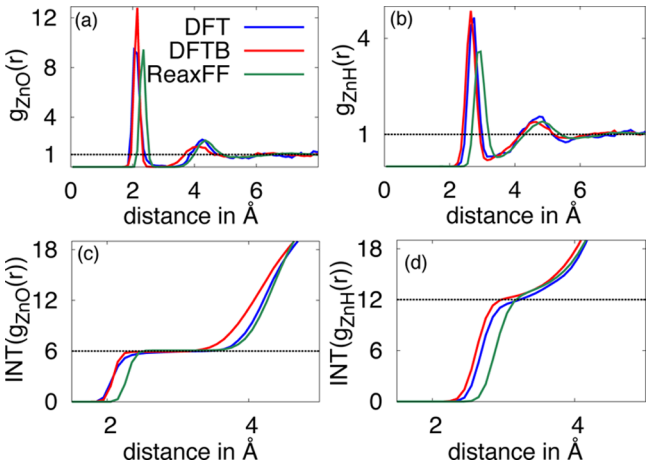

Figure 1. Radial distribution functions (RDF) for (a) Zn^{2+}–$O(H_2O)$ and (b) Zn^{2+}–$H(H_2O)$ obtained in DFT, DFTB, and ReaxFF MD simulations. The corresponding RDF integrals are depicted in (c) and (d).

dx.doi.org/10.1021/ct3007106 | J. Chem. Theory Comput. 2012, 8, 4517–4526

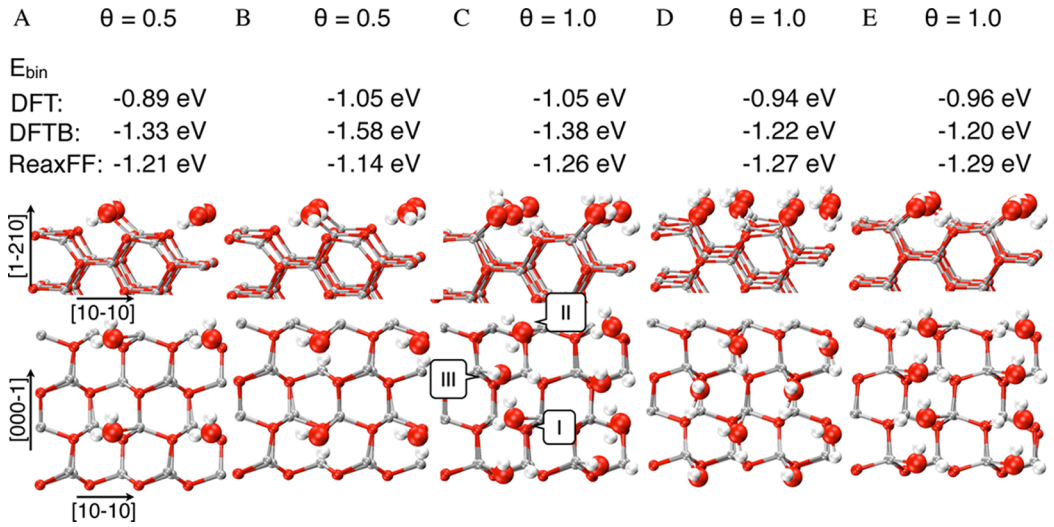

Figure 2. Five adsorption configurations and corresponding binding energies (DFT, DFTB, ReaxFF) of water on ZnO($1\bar{2}10$) (side and top views) at different water coverages θ. Configurations A and B differ in the number of hydrogen bonds formed to the surface. Configurations C, D, and E correspond to half-dissociated, undissociated, and fully dissociated water monolayers. In configuration C, different adsorbing states of water are labeled with roman numerals (see text).

well-suited to investigate also the adsorption of water on the ($1\bar{2}10$) surface.

2.3. ZnO($1\bar{2}10$) Surface Model. The ($1\bar{2}10$) surface is modeled as a periodically repeated slab with a thickness of 12 Å, which corresponds to 4 layers of ZnO, separated by a vacuum or bulk liquid water layer of 15 Å in the z direction perpendicular to the surface. For the DFT and DFTB simulations, we use a (2 × 2) surface cell in the xy plane, with a surface area of 11.4 × 10.6 Å^2. For the ReaxFF simulations, we use a larger (4 × 4) surface cell.

Geometry optimization of the ($1\bar{2}10$) surface slab results in an inward relaxation of the zinc surface ions involving a decrease of the zinc oxygen bond length from 2.00 to 1.89 Å, leading to a tilted Zn−O dimer structure.[11] The calculated surface energy in the absence of any additional water molecule is 0.84 J/m^2, in close agreement with the previously computed PBE value of 0.85 J/m^2.[11] The corresponding surface energies at the DFTB and ReaxFF levels are 0.73 and 1.45 J/m^2, respectively (Table 1). The large deviation of the ReaxFF from the PBE value may be in part explained by the fact that the force field parameters were fitted to DFT calculations using the B3LYP xc functional (unlike the DFTB parametrization, which is based on PBE references). In fact, it is well-known that GGA calculations tend to underestimate surface energies as compared to LDA or B3LYP values.

2.4. Coverage Definition. We define the coverage factor of water on the ($1\bar{2}10$) surface as $\theta = (N_{H_2O}/N_{Zn})$, where N_{H_2O} and N_{Zn} denote the numbers of adsorbed water molecules and of possible Zn binding sites on the surface area of the simulation cell. With this definition, a coverage θ = 1.0 ML corresponds to 8 water molecules for the (2 × 2) surface model (DFT and DFTB simulations) and to 32 molecules for the (4 × 4) model (ReaxFF simulations).

3. RESULTS

3.1. Solvated Zn^{2+} Ion. To get a first indication of the performance of the DFT, DFTB, and ReaxFF approaches in describing the interaction between zinc and water, we first consider a single, solvated Zn^{2+} ion. The ion is placed in a cubic box with edge-length of 12 Å filled with 66 water molecules for DFT and DFTB calculations and an edge-length of 24 Å filled with 548 water molecules for reactive force field calculations. The system is heated to 300 K, and a 4 ps constant-temperature MD simulation is carried out for each of the three methods, from which radial distribution functions (RDF) of the Zn−O and Zn−H atom pairs can be calculated (Figure 1a and b). The first peak in the Zn−O RDF is centered at 2.15 Å for both the DFT and the DFTB simulations, whereas it is shifted 0.2 Å away from the Zn ion when using ReaxFF. The experimentally determined Zn−O distance for the first hydration shell around a single Zn^{2+} ions is 2.09 Å.[28] All three theoretical results therefore slightly underestimate the Zn−O interaction, resulting in a 3−4% longer bond distance. The position of the second RDF peak, corresponding to the second hydration shell around the ion, is, as expected, less intense but wider for all three methods. While for DFT and ReaxFF simulations the second peak lies at about 4.3 Å, DFTB predicts a second maximum located 0.2 Å closer to the Zn ion. Similar trends in the RDFs can be observed taking into account the Zn−H pair. The peaks are located at 2.76 and 2.65 Å for DFT and DFTB, whereas ReaxFF predicts a slightly larger distance of 2.9 Å for the Zn−H bond in the first hydration shell, similarly as for the Zn−O bond. In the second hydration shell, again DFTB leads to a 0.2 Å smaller Zn−H distance than do DFT and ReaxFF.

The integrals of the RDFs, corresponding to the number of coordinating water ligands around the Zn^{2+} ion, are reported in Figure 1c and d for Zn−O and Zn−H, respectively. All three methods show a distinct plateau at a coordination of 6 water molecules, especially visible taking into account the Zn−O RDF. This agrees well with the diffraction and EXAFS experiments performed for solvated Zn^{2+} ions by Ohtaki and Radnai,[28] which reveal the presence of 6 water molecules in the first hydration shell. In conclusion, despite the small differences highlighted above, all three simulation methods give a reliable description of the bonding interactions between single Zn^{2+} ions and water. This is a good basis to proceed with the study of the hydration of the ZnO($1\bar{2}10$) surface, as presented in the next section.

3.2. Monolayer Adsorption. We begin the investigation of the ZnO($1\bar{2}10$)/water interface with DFT calculations to determine the most stable configurations of adsorbed water, from a single molecule to a full monolayer (ML). The obtained ML geometries and adsorption energies are then compared to the results of the DFTB and ReaxFF methods. In doing this, we follow an ab initio thermodynamics approach that allows us to predict the most stable adsorption coverages as a function of temperature and water vapor pressure.

3.2.1. DFT Results. To determine the stable adsorption configurations of water molecules on the (2 × 2) surface cell, we first perform a short (2 ps) MD simulation at 300 K, followed by geometry optimization. Placing a single H_2O molecule in the cell (whose size is large enough to prevent interactions with its neighbor images through the periodic boundary conditions), we obtain two (meta)stable adsorption configurations out of five independent MD runs, with adsorption energies of 0.88 and 1.02 eV per molecule, respectively. The same two configurations are retained increasing the coverage θ from 0.125 to 0.5 ML, that is, including 3 molecules in the simulation cell (Figure 2). The binding energies vary only negligibly with respect to θ = 0.125, amounting to 0.89 and 1.05 eV/H_2O for A and B, respectively, indicating no intermolecular interactions occurring at this small coverage. The two configurations differ only in the number of hydrogen bonds to the surface, the molecule forming in both cases a strong bond to a surface Zn atom via the O atom (OW). In configuration A, the water molecule bridges two Zn−O dimer trenches in the ZnO surface by forming a hydrogen bond between one of the hydrogen atoms (HW) and a surface oxygen atom (OS) across the trenches. In configuration B, the adsorption is further stabilized by a second hydrogen bond to another OS atom along the dimer trench (see Figure 2A,B). Upon adsorption, the overall surface morphology remains unchanged, while the tilt angle of the Zn−O dimer at the OW−Zn interaction site is relaxed back to the bulk positions. This is easily explained in terms of the recovered tetrahedral coordination of the Zn surface atom by three OS and one OW atoms, as in bulk ZnO.

Increasing the coverage further to 1 ML, we observe partial or complete dissociation of the adsorbed water molecules. In particular, we obtain three different adsorption configurations of the ML, depicted in Figure 2C−E. In the most stable configuration C (average adsorption energy of 1.05 eV/H_2O), every second water molecule is dissociated, leading to a shortening of the OW−Zn distance by about 0.1 Å. This dissociative adsorption mode (indicated with III in Figure 2C) leads to an OH group bound to a Zn site and a proton bound to a neighbor OS atom across the trench in the ($10\bar{1}0$) direction. The molecularly adsorbed molecules adopt two different geometries (indicated with I and II in Figure 2C). Geometry I resembles the configuration A at low coverage, with one additional hydrogen bond to a next-neighbor adsorbed OH group. In geometry II, the water molecule forms two hydrogen bonds to its two neighboring OH groups. The adsorption configuration C can be thus described as a stacking order of dissociated and molecularly adsorbed water, in which two different molecularly adsorbed geometries alternate.

In the two further configurations, lying about 0.1 eV/H_2O higher in energy, all water molecules building the ML are dissociated (Figure 2D,E). In D the molecules dissociate along the Zn−O dimer trenches, and the two resulting OH groups are bridged by one H bond without further interactions between different dissociated molecules. In E the dissociation occurs across the trenches, leading to the formation of a fully developed hydrogen-bond network between the adsorbed OH groups. This fully dissociated H-bond network has been proposed by Raymand et al.[14] to be the most stable adsorption configuration at θ = 1.0 ML. Our computed binding energies instead suggest that the half-dissociated configuration C is the most stable at the level of PBE-DFT.

The different types of chemical bonds that occur at the ZnO($1\bar{2}10$)/water interface are investigated by plotting the projected density of states (PDOS) of two different adsorption scenarios (configurations C and E) in comparison with the clean surface and an isolated water molecule (Figure 3). In the upper part of the figure, we report the DOS projections on the s and p orbitals of the OW atoms along with the projections on the s and d orbitals of Zn. Evident is the localization of the bonding OW-s orbitals at about −20 eV and the large overlap between the Zn-d and the OW-p orbitals at about −5 eV. The latter leads to a more pronounced splitting of the Zn-d peak with respect to the clean surface and to a broadening of the OW-p peaks over the whole valence band, as a consequence of the Zn−O bond formation. It is interesting to note the differences between the molecularly adsorbed water in C(I) and C(II) and the dissociatively adsorbed water in C(III) and E. In the dissociative adsorption case, the OW-s orbital is localized at about 1.3 eV higher energy, and a pronounced OW-p peak appears at the top of the valence band, as expected from the presence of an electron lone-pair on the adsorbed OH group.

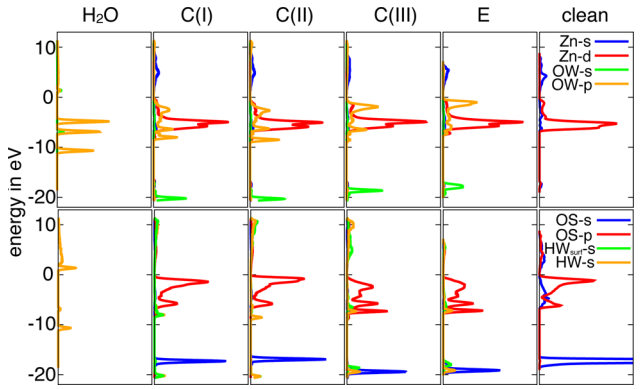

Figure 3. Projected density of states (PDOS) of selected monolayer configurations C and E (see Figure 2) as compared to the isolated water molecule and the clean ZnO($1\bar{2}10$) surface.

Differences between the molecularly and dissociatively adsorbed modes are also visible from the analysis of the OS-s and OS-p together with the HW-s orbitals (lower part of Figure 3). While no evident changes in the PDOS are associated with the formation of a water-surface hydrogen bond (panels C(I) and C(II) as compared to the clean surface), the transfer of a proton from the water to the surface leads to a restructuring of the OS-p band. It leads to a decrease of the peak at the valence-band edge as a consequence of (partial) saturation of the dangling bond of the surface O atom, and appearance of a sharp double-peak at the bottom of the valence band, indicative of the formation of a covalent OS-H bond. This also causes a shift in the OS-s peak to lower energy values (analogous to the shift of the OW-s peak between the dissociated and molecular case, as described above).

dx.doi.org/10.1021/ct3007106 | J. Chem. Theory Comput. 2012, 8, 4517−4526

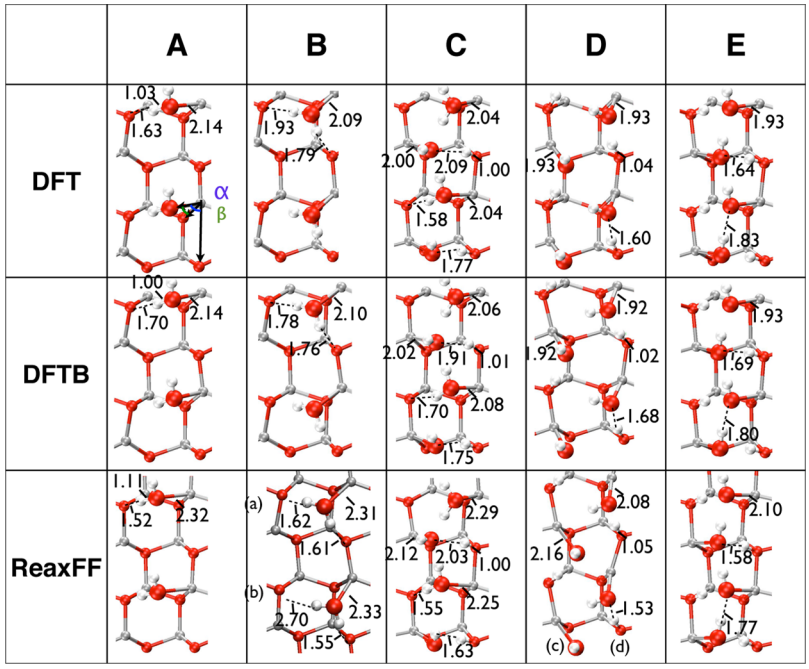

Figure 4. Overview of the average bond lengths of the thermodynamically most stable (half) monolayer geometries as introduced in Figure 2 calculated with DFT, DFTB, and ReaxFF molecular dynamics simulations (top view). The values of the angles α and β are reported in Table 1.

Table 2. Average Bond Angles (As Defined in Figure 4) for the Thermodynamically Most Stable (Half) Monolayer Geometries of Water over ZnO($1\bar{2}10$) (See Figure 2) Calculated with DFT, DFTB, and ReaxFF

	A			B		
	DFT	DFTB	ReaxFF	DFT	DFTB	ReaxFF
α	96.88	96.65	102.74	90.67	88.25	(a) 89.98 (b) 97.56
β	81.03	75.46	88.20	55.29	53.86	(a) 52.33 (b) 50.08

	C(i)			C(ii)			C(iii)		
	DFT	DFTB	ReaxFF	DFT	DFTB	ReaxFF	DFT	DFTB	ReaxFF
α	101.87	99.99	109.05	106.09	100.83	1117.19	102.97 (1HB) 105.33 (2HB)	103.08	108.87 (1HB) 117.73 (2HB)
β	92.30	86.41	93.66	83.53	79.58	79.79	83.45	80.83	88.93

	D			E		
	DFT	DFTB	ReaxFF	DFT	DFTB	ReaxFF
α	107.18	105.42	(c) 98.05 (d) 118.45	101.95	104.64	111.37
β	50.42	53.47	(c) 53.55 (d) 51.84	89.52	88.02	91.24

3.2.2. Comparison to DFTB and ReaxFF. Starting from the adsorption configurations obtained with DFT, we now perform further geometry optimizations with DFTB and ReaxFF and compare the results with the DFT reference. A detailed overview of the obtained relaxed geometries for selected coverages is reported in Figure 4 and Table 2. In all systems, the Zn−OW bond lengths calculated with DFTB nicely match the DFT results, with only small deviations of about 0.02 Å. The average Zn−OW distance of 2.14 Å agrees well with the peak position of the RDF of the hydrated Zn^{2+} ion (2.15 Å) discussed in section 3.1. At the ReaxFF level, the computed Zn−OW bond lengths are systematically longer by 0.2 Å, which also corresponds to the results of the RDF analysis (Figure 1).

The lengths of the hydrogen bonds formed between the HW and OS atoms exhibit larger deviations from the DFT reference, of the order of 0.1 Å for DFTB and up to 0.3 Å for ReaxFF. In particular, ReaxFF tends to overestimate the hydrogen-bond strength between surface and adsorbed water with respect to PBE-DFT, which may be consistent with the larger surface energy of the clean ($1\bar{2}10$) plane. Accordingly, as a consequence of the stronger H-bonds, the angles between the Zn−OW bonds and the surface plane (defined as α and β in Figure 4 and Table 2) also present considerable deviations from the corresponding DFT values. This results in slightly different ordering and alignment of the adsorbed water molecules over the surface at low coverage ($\theta = 0.5$), especially for the ReaxFF approach. In particular, in the adsorption configuration B, ReaxFF yields two geometries of molecularly adsorbed water (labeled with (a) and (b) in Figure 4 Table 2). One of the molecules (a) forms two hydrogen bonds with the surface, as in

dx.doi.org/10.1021/ct3007106 | J. Chem. Theory Comput. 2012, 8, 4517−4526

the DFT reference and in the DFTB structure. The second molecule (b) adopts a configuration where only one hydrogen bond forms along the Zn−O dimer trench. Because of the short H-bonds, the two molecules bend considerably toward the surface plane, leading to a highly distorted coordination of the surface Zn atoms they are bound to. At θ = 1.0, the hydrogen-bonding networks in C, D, and E do not change their overall patterns after DFTB or ReaxFF optimization, although their relative energetic stability does change, as explained below.

We quantify the relative energetic stability of the various adsorption scenarios by means of differences in the Gibbs free energy $\Delta\gamma$ of the water-adsorbed surfaces with respect to the clean surface. This can be computed as:[16]

$$\Delta\gamma = \frac{1}{N_C A}(E_{slab}^{H_2O/ZnO} - E_{slab}^{ZnO} - N_{H_2O}(E_{single}^{H_2O} + \Delta\mu_{H_2O})) \quad (1)$$

where N_C is the number of surface unit cells, A is their surface area, and N_{H_2O} is the number of water molecules. E_{slab}^{ZnO} and $E_{slab}^{H_2O/ZnO}$ are the computed total energies of the slab in the clean and adsorbed states. $\Delta\mu_{H_2O}$ defines the chemical potential of the water vapor with respect to an isolated water molecule with computed energy $E_{single}^{H_2O}$:

$$\Delta\mu_{H_2O} = \Delta\tilde{\mu}_{H_2O} + k_B T \ln\frac{p}{p_0} \quad (2)$$

where p and T are the vapor pressure and temperature, k_B is the Boltzmann constant, and $\Delta\tilde{\mu}_{H_2O}$ contains the entropy and enthalpy variation of the vapor gas at the reference pressure p_0, as available in standard thermodynamical tables.[29] In our analysis, we assume constant water vapor pressures p = 1.0 bar and $p = 10^{-10}$ bar, and report in Figure 5 the surface energy values as a function of the temperature for the DFT, DFTB, and ReaxFF calculations at θ = 0.5 and θ = 1.0 ML.

The DFT results predict a coverage of 1.0 ML with adsorption configuration C to be the most stable surface structure at temperatures lower than 520 K for p = 1.0 bar and lower than 291 K for $p = 10^{-10}$ bar (Figure 5a). At higher temperatures, desorption of the whole ML takes place, leaving a clean surface. The coverage of 0.5 ML is never favorable, and the corresponding free energy curve intersects the one associated with the clean surface at the same point as the 1.0 ML curve. This is a consequence of the equal average adsorption energies per molecule computed for θ = 0.5 and 1.0 ML (see Figure 2).

The DFTB approach likewise predicts the monolayer configuration C to be the most stable structure at low temperatures. However, differently from the DFT reference, it also predicts an interval of stability for the 0.5 ML structure (between 600 and 780 K at 1.0 bar, or between 330 and 438 K at 10^{-10} bar (Figure 5b)). This reflects the higher average binding energy per molecule computed with DFTB at θ = 0.5 ML with respect to θ = 1.0 ML (see Figure 2). At the ReaxFF level of approximation, we obtain, as in the DFT case, a direct transition from the full ML to the clean surface, with transition temperatures of 620 and 360 K at 1.0 bar and 10^{-10} bar, respectively. The 0.5 ML structure is less stable than in the DFT case, due to the lower average adsorption energy per molecule obtained at the lower coverage. Moreover, the free energy curves corresponding to the three ML configurations C, D, and E are almost degenerate, with a slight preference for the fully dissociated structure (see inset of Figure 4c).

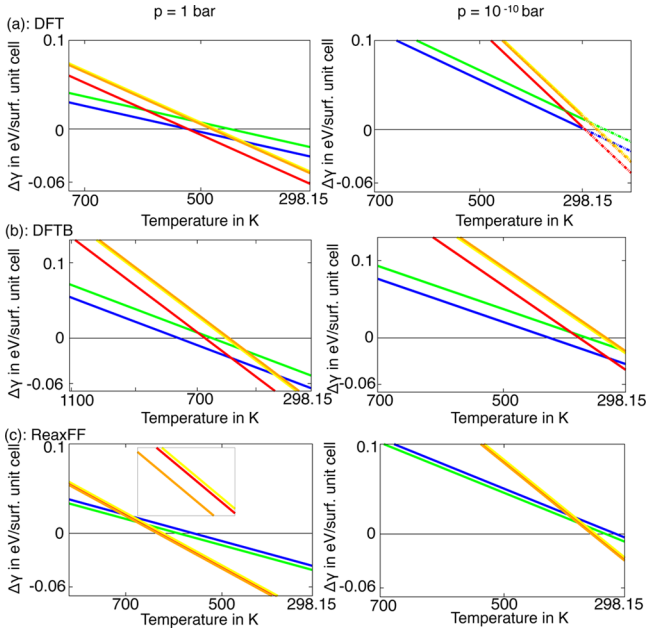

Figure 5. Dependencies of the Gibbs free energy of the ZnO($1\bar{2}10$) surface at various water coverages on the water vapor chemical potential obtained with (a) DFT, (b) DFTB, and (c) ReaxFF. The blue and green lines correspond to configurations A and B in Figure 2 (0.5 ML), and the red, yellow, and orange lines to configurations C, D, and E (1.0 ML). The data below 298 K in the top-right panel (dotted lines) are obtained from a linear extrapolation of the higher temperature curves.

3.3. Influence of Bulk Water. After the investigation of the interface between ZnO($1\bar{2}10$) and water vapor up to a coverage of 1 ML, we now study the dynamical behavior of the surface placed in contact with bulk, liquid water. To this aim, we fill the vacuum region between the periodically repeated surface slabs with H_2O molecules at the normal density of about 1 g/cm^3. As a first investigation, we start from a surface decorated with only 0.5 ML of adsorbed water and randomly placed water molecules in the liquid bulk, and monitor the time evolution of the average coordination number (CN_{Zn-OW}) of the surface Zn atoms in MD simulations with the three simulation methods, DFT, DFTB, and ReaxFF. As at the beginning of the simulations only one-half of the Zn sites are bound to water molecules, CN_{Zn-OW} starts at the value of 0.5. Within a few picoseconds of MD at 300 K, however, CN_{Zn-OW} increases and stabilizes at about 1.0 for all three methods, indicating full occupation of the Zn surface site by one (and only one) water molecule. Importantly, no further increase of the coordination number is observed over a much longer simulation time (tens of ps) in DFTB and ReaxFF simulations.

We now analyze the propensity of dissociative versus molecular water chemisorption in the presence of bulk liquid water with the three methods, which predicted different adsorption configurations at the coverage of 1 ML (see Figure 2). Starting from three different initial configurations of the chemisorbed layer, (i) fully dissociated, (ii) half-dissociated, and (iii) nondissociated, we perform at least 10 ps long MD runs of the systems in contact with bulk water. Longer simulations are performed for DFTB (30 ps) and ReaxFF (1000 ps). The time evolution of the average coordination number $CN_{OW(s)-HW}$ of the chemisorbed OW atoms to hydrogen atoms are shown in Figure 6 for all investigated

dx.doi.org/10.1021/ct3007106 | J. Chem. Theory Comput. 2012, 8, 4517−4526

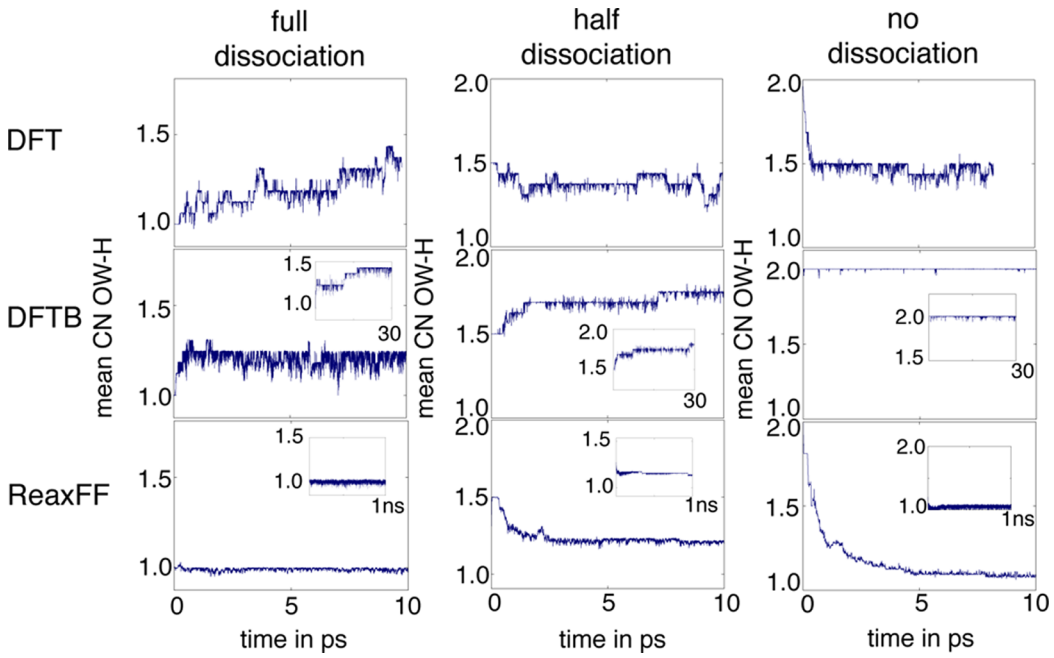

Figure 6. Time evolutions of the mean coordination numbers of water oxygen and hydrogen over the ZnO($1\bar{2}10$) surface obtained in MD simulations starting from three different initial structures: full dissociation (left), half dissociation (center), and no dissociation (right). Each row shows the results of the DFT, DFTB, and ReaxFF methods (top to bottom).

cases. The three initial conditions used correspond to $CN_{OW(s)-HW}$ equal to (i) 1.0, (ii) 1.5, and (iii) 2.0, respectively, at the beginning of the MD simulations.

At the DFT level, irrespective of the initial conditions, within 10 ps an equilibrium configuration of half-dissociated water molecules is reached. Notably, the recombination of the initially fully dissociated water (increase of $CN_{OW(s)-HW}$ from 1.0 to 1.5) takes much longer than the (half) dissociation of the molecularly adsorbed layer, which is completed in less than 100 fs (Figure 6, top three panels). The structure of the chemisorbed water layer at the end of the simulations corresponds to the adsorption configuration C in Figure 2; that is, every second water molecule is dissociated.

The ReaxFF simulations show a different trend, in which complete dissociation of the adsorbed water molecules ($CN_{OW(s)-HW}$ = 1.0) is obtained at the end of the simulations. After starting from a half-dissociated chemisorbed layer, an average value $CN_{OW(s)-HW}$ = 1.2 is obtained after 1000 ps, most probably indicating the presence of a local energy minimum in which a few of the adsorbed molecules remain undissociated. Interestingly, however, when starting from undissociated water, complete dissociation takes place very rapidly, within 10 ps. Therefore, ReaxFF predicts the same adsorption configuration to be stable both at 1 ML of water vapor and in the presence of liquid water (fully dissociated configuration E in Figure 2). This result is consistent with a previous ReaxFF investigation of the water adsorption on the ($1\bar{2}10$) ZnO surface performed by Raymand et al.[17]

DFTB predicts the opposite scenario. The molecularly adsorbed layer is remarkably stable over more than 30 ps of MD ($CN_{OW(s)-HW}$ = 2.0). Also, starting with a half-dissociated or fully dissociated chemisorbed layer, a slow but evident increase of $CN_{OW(s)-HW}$ toward values higher than 1.5 is observed on the time scale of the simulation (which would probably end up with $CN_{OW(s)-HW}$ = 2.0 at longer times). The MD simulations thus indicate a net preference of the DFTB method for molecular adsorption in the presence of bulk water, which is in contradiction with the results at θ = 1.0 ML, where a half-dissociated structure is favorable (see Figures 2 and 5). Therefore, the stabilization of molecular water in the chemisorbed layer must be due to the formation of a developed hydrogen-bonding network above the surface, resulting in different dissociation equilibria within the DFTB formalism.

A possible explanation for this behavior may be associated with the changes of the self-consistent charges (SCC) of the atomic species under the different adsorption conditions. Consistently with typical literature values,[30] the SCC on the O atoms amounts to −0.78 e in bulk water, and decreases in value to −0.60 e after molecular adsorption on the surface, becoming closer to the SCC of surface O atoms (−0.5 e). Instead, the Zn−O bonds in the ReaxFF formalism are more strongly polarized, with a surface O point charge of −0.90 e, consistently with the high surface energy values computed in section 2.3. It can be thus inferred that the markedly different behavior of water on the ZnO surface in the DFTB and ReaxFF formalism may arise, at least in part, from the large difference in the electrostatic interactions between atomic charges in the two cases.

An important consequence of different dissociation equilibria at the interface is the different structuring of water layers in surface proximity predicted by the three formalisms. In Figure 7, the density of OW and HW atoms averaged over 10 ps MD simulations performed with the equilibrium structures of Figure 6 is plotted against the height z above the surface plane. For ReaxFF, the first HW peak at 1.0 Å corresponds to the dissociated protons covalently bond to the OS atoms. The first OW and the second HW peaks (at 1.5 and 2.3 Å) arise from the adsorbed OH groups in an almost vertical orientation. The two further well-defined OW peaks and the associated HW peaks between 2.8 and 4.5 Å indicate the presence of a second and a third strongly structured water layer over the surface. This structuring is much less pronounced at the DFTB level,

dx.doi.org/10.1021/ct3007106 | J. Chem. Theory Comput. 2012, 8, 4517−4526

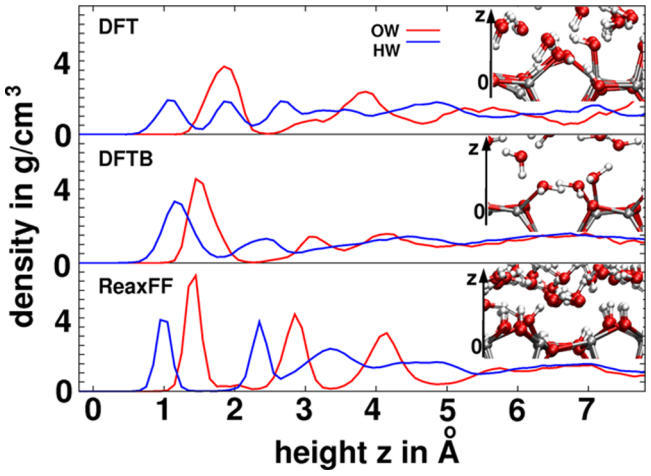

Figure 7. Density of OW and HW atoms of liquid water against the height z above the ZnO($1\bar{2}10$) surface obtained in MD simulations using DFT (top), DFTB (middle), and ReaxFF (bottom). To improve the comparison, the HW density is multiplied by a factor of 10. The zero point of z is set at the position of the surface Zn atoms. For each method, the inset displays a snapshot of the equilibrium interface structure.

where the first HW and OW peaks at 1.2 and 1.5 Å reflect the presence of water molecules bent with the hydrogen atoms toward the surface in the molecularly adsorbed layer. The second HW peak at 2.4 Å arises both from molecules adsorbed in an upright geometry and from H atoms of the second water layer. Both this second and a third water layer are visible in the OW density distribution, although with very small density maxima. The density obtained from DFT MD shows two distinct maxima and an intermediate subsidiary peak for OW, and three distinct peaks for HW. The first OW peak at 2.0 Å is broadened, as it represents both the molecular and the dissociated adsorbed water molecules of the interface layer. The HW peaks at 1.1, 2.0, and 3.7 Å depict the HW atoms bonded directly to the surface, forming a hydrogen bond to a OS or a neighboring OW and pointing away from the surface, respectively. The overall amount of structuring predicted by DFT extends up to about 4.5 Å over the surface, with intensities intermediate between the ReaxFF and the DFTB methods.

As a final test of the performance of the two approximate methods, we study the reaction between liquid water and a neutral surface vacancy defect, obtained upon removal of a Zn−O dimer from the ($1\bar{2}10$) surface. Starting from randomly placed water molecules over the dry defective surface (Figure 8a), MD simulations performed with either DFTB or ReaxFF predict the same reaction mechanism and final outcome (Figure 8b and c, respectively). Within a few picoseconds, the under-coordinated subsurface Zn and O atoms become saturated by an OH and an H group, respectively, as a consequence of the dissociative adsorption of a water molecule. Moreover, one of the O atoms neighbor to the Zn vacancy receives a proton from the bulk liquid. Notably, in this case, also DFTB, not only ReaxFF, predicts water dissociation at the vacancy site and increased reactivity (basicity) of the O atoms nearby, indicating that the subtle differences between the methods in the case of protonation equilibria of defect-free surfaces are not as substantial as to predict a different behavior in the case of obvious defects.

4. DISCUSSION

A reliable description of the ZnO/water interface in MD simulations is fundamental to study the atomistic details governing the behavior of ZnO nanoparticles in a wet environment. In particular, the precise structure of the water layers in proximity of oxide/water interfaces has been observed to be a very important component of the driving force for the adhesion of proteins.[31−35] It has also been suggested that the specific recognition of materials by short peptide sequences arises, at least in part, from the sensing of the local density variation of water at the solid/liquid interface at the molecular level.[36] Moreover, the dissolution of ZnO nanoparticles, which is most probably the cause of their toxicity both in single cells and in higher animals,[20] obviously depends on the hydration structure of the solvent-exposed surface.

DFT-based simulations can be considered as a reliable tool to predict the hydration structure of surfaces, although the choice of the xc functionals may have a non-negligible influence on the simulations' outcome.[37] However, the small system size and especially the limited simulation time accessible with DFT-based MD prevent a statistically relevant exploration of the phase-space, as required in investigations of protein adsorption or surface dissolution processes. We have thus performed a comparison between a standard DFT implementation (plane-wave, ultrasoft pseudopotentials, PBE xc functional), the semiempirical, DFT-based tight-binding approach DFTB, and a recently published reactive force field for ZnO/water interfaces (ReaxFF) to assess their performance in describing

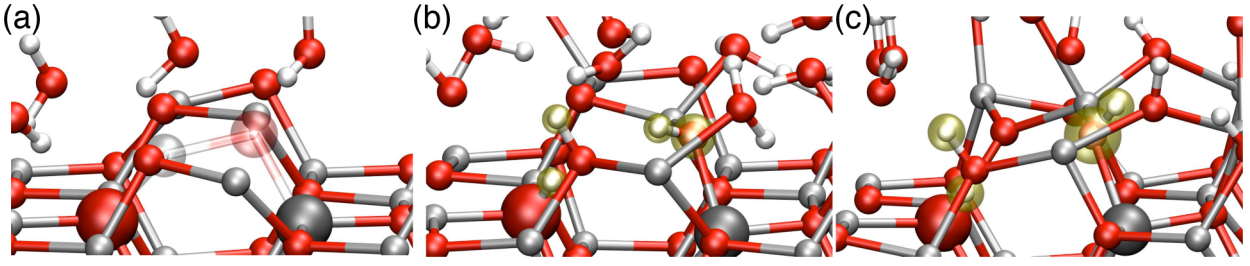

Figure 8. Snapshots from MD simulations of the reaction between the ZnO($1\bar{2}10$) surface and liquid water, including a missing Zn−O dimer as a surface defect. (a) Initial configuration. The missing Zn and O atoms are rendered as semitransparent, and the resulting under-coordinated subsurface atoms are highlighted as larger spheres. (b) Final configuration after 15 ps of MD using DFTB. (c) Final configuration after 15 ps of MD using ReaxFF. Both simulation methods show the same qualitative reaction mechanism, dissociative adsorption of a water molecule at the uncoordinated subsurface sites and protonation of one of the surface O atoms neighboring the initial defect. The newly adsorbed H and OH groups are highlighted with a yellow halo.

the nonpolar ZnO($1\bar{2}10$) surface in contact with water vapor and water liquid.

All three methods describe the interactions between a single Zn^{2+} ion and liquid water in acceptable agreement with experimental results. However, they are found to predict different adsorption structures for a water monolayer adsorbed on the surface. DFT and DFTB predict a half-dissociated structure to be most stable, while ReaxFF predicts a fully dissociated (hydroxylated) structure. In contact with bulk liquid water, the half-dissociated and the fully dissociated structures remain stable within DFT and ReaxFF, respectively, while recombination of the dissociated water with formation of a molecularly adsorbed first water layer takes place at the level of DFTB. This finding is peculiar, because previous theoretical studies on ZnO and other metal oxides indicate, generally, a tendency toward dissociation of the chemisorbed layer promoted by higher water coverages.[17] The obtained tendency of the water to recombine in the DFTB simulations might be due to the intrinsic shortcomings of the used self-consistent-charge approach to describe proton affinities and binding energies. In this approach, the Taylor series of the total energy of the system expanded in terms of the density is truncated after the second term (second-order tight-binding). As a consequence of this approximation, the proton affinities of negatively charged molecules are overestimated due to an overbinding of the O−H bond of about 6−7 kcal/mol.[38] Gaus et al. suggested that the problem can be solved when third-order terms are included in the series expansion of the tight-binding energy,[38] which could be performed in future works for the whole ZnO/water interface system.

The ReaxFF approach offers in principle a viable alternative to both DFT and DFTB, with a nice compromise between accuracy and computational cost. In the case of the ZnO($1\bar{2}10$) surface, however, ReaxFF predicts a different water structure with respect to our DFT reference, as mentioned above. In the absence of specific experimental information, which is available only for the other nonpolar surface ($10\bar{1}0$),[15] it remains unclear what is the correct adsorption structure, and what is the influence of the chosen xc functional on the DFT results. In the case of the ($10\bar{1}0$) surface, the ReaxFF results available in the literature nicely match both PBE-DFT and experiments findings, predicting 50% of the adsorbed water molecules to dissociate at θ = 1.0 ML. At higher coverages, the amount of dissociation increases to about 80% for the ($10\bar{1}0$) surface and 100% for the more stepped ($1\bar{2}10$) surface.[17] A reason for the observed behavior may be the much stronger polarization of the ZnO bond in ReaxFF than in DFTB, as evident from the analysis of point charges presented in section 3.3. This difference, together with the different polarizabilities of the first water layer, may shift the hydroxylation equilibrium toward dissociative adsorption. In line with these observations, we note that the overestimated ReaxFF surface energy of the clean ($1\bar{2}10$) surface with respect to PBE-DFT (1.45 vs 0.84 J/m^2, see Table 1) is also an indication of overestimated surface reactivity. In fact, surfaces with lower surface energies show a tendency for molecular adsorption, whereas surfaces with higher energy show a stronger hydroxylation equilibrium caused by water dissociation.[39,40] Consistently, DFTB predicts both the lowest surface energy (0.79 J/m^2) and stable molecular adsorption.

Despite the shortcomings and inconsistencies highlighted above, we have to note that the energy differences associated with the different adsorption structures are rather small (less than 0.1 eV for a binding energy per molecule of about 1 eV). Therefore, little changes of the computational parameters (xc functionals and pseudopotentials in DFT, Slater-Koster parameters in DFTB, numerical parameters in ReaxFF) may easily result in an altered hydroxylation equilibrium, especially in the presence of bulk water. In our opinion, this points toward nearly equal stabilities of the molecularly adsorbed and dissociated water molecules of the ZnO($1\bar{2}10$) surface. We could therefore speculate that the extent of water dissociation in the adsorbed layer may have no or only very little influence on the energy barriers associated with the dissolution of Zn^{2+} ions out of surface edges. ReaxFF may thus be a good choice of simulation method to study this kind of phenomena, as it would allow a statistically relevant estimation of the free-energy profile associated with the dissolution reactions. In fact, our preliminary results about the reaction of liquid water with a neutral surface defect (see Figure 8) are encouraging, demonstrating qualitatively the same outcome of MD simulations performed with either DFTB or ReaxFF.

An important consequence of the different hydroxylation equilibria is the different structuring of the water layers up to about 5.0 Å above the surface (see Figure 7). As this structure has been found to considerably influence the geometry, adsorption energy, and adhesion forces of biomolecules at solid/liquid interfaces,[31,36,41] the choice of the simulation method may heavily affect atomistic simulations between ZnO and dissolved biomolecules. Therefore, as long as a reactive force field to describe at the same time the chemistry of dissolved amino acids and ZnO surfaces is still missing, effort should be spent on assessing the viability of the DFTB method for future investigations of biohybrid ZnO interfaces requiring longer simulation times and larger system sizes than accessible by DFT. In particular, its predictive power for this specific case shall be carefully checked in future works in comparison with full quantum mechanical MD simulations.

AUTHOR INFORMATION

Corresponding Author

*E-mail: colombi@hmi.uni-bremen.de.

Notes

The authors declare no competing financial interest.

ACKNOWLEDGMENTS

We wish to thank Andreia da Rosa, Ney Moreira, Christof Köhler, Bálint Aradi, and Tino Wolter for discussions regarding the ZnO model and the DFTB setup; Bernd Meyer for providing us with his pseudopotentials; and Lutz Mädler for the initial motivation tfor this work. Computational resources have been allocated at the BCCMS and at the HLRN computing center (Hannover-Berlin, Germany). We acknowledge funding from the APF project "Func-Band" of the Land Bremen and the EU-FP7-NMP grant 229205 "ADGLASS".

REFERENCES

(1) Gupta, S. K.; Joshi, A.; Kaur, M. *J. Chem. Sci.* **2010**, *122*, 57−62.
(2) Baxter, J. B.; Aydil, E. S. *Appl. Phys. Lett.* **2005**, *86*, 1−3.
(3) Yadav, B.; Srivastava, R.; Dwivedi, C.; Pramanik, P. *Sens. Actuators, B* **2008**, *131*, 216 −222.
(4) Jung, H.; Choi, H. *Appl. Catal., B* **2006**, *66*, 288 −294.
(5) Vayssieres, L. *Adv. Mater.* **2003**, *15*, 464−466.
(6) Yi, G.-C.; Wang, C.; Park, W. I. *Semicond. Sci. Technol.* **2005**, *20*, S22−S34.

(7) Tani, T.; Mädler, L.; Pratsinis, S. E. *J. Nanopart. Res.* **2002**, *4*, 337−343.
(8) Hoppe, R. *Naturwissenschaften* **1967**, *54*, 587−588.
(9) Scarano, D.; Spoto, G.; Bordiga, S.; Zecchina, A.; Lamberti, C. *Surf. Sci.* **1992**, *276*, 281 −298.
(10) Zhang, P.; Xu, F.; Navrotsky, A.; Lee, J. S.; Kim, S.; Liu, J. *Chem. Mater.* **2007**, *19*, 5687−5693.
(11) Meyer, B.; Marx, D. *Phys. Rev. B* **2003**, *67*, 01−11.
(12) Moreira, N. H.; Dolgonos, G.; Aradi, B.; da Rosa, A. L.; Frauenheim, T. *J. Chem. Theory Comput.* **2009**, *5*, 605−614.
(13) Raymand, D.; van Duin, A. C.; Baudin, M.; Hermansson, K. *Surf. Sci.* **2008**, *602*, 1020 −1031.
(14) Raymand, D.; van Duin, A. C.; Spångberg, D.; Goddard, W. A.; Hermansson, K. *Surf. Sci.* **2010**, *604*, 741 −752.
(15) Meyer, B.; Marx, D.; Dulub, O.; Diebold, U.; Kunat, M.; Langenberg, D.; Wöll, C. *Angew. Chem., Int. Ed.* **2004**, *43*, 6641−6645.
(16) Meyer, B.; Rabaa, H.; Marx, D. *Phys. Chem. Chem. Phys.* **2006**, *8*, 1513−1520.
(17) Raymand, D.; van Duin, A. C.; Goddard, W. A.; Hermansson, K.; Spångberg, D. *J. Phys. Chem. C* **2011**, *115*, 8573−8579.
(18) Cooke, D. J.; Marmier, A.; Parker, S. C. *J. Phys. Chem. B* **2006**, *110*, 7985−7991.
(19) Calzolari, A.; Catellani, A. *J. Phys. Chem. C* **2009**, *113*, 2896−2902.
(20) Xia, T.; Kovochich, M.; Liong, M.; Mädler, L.; Gilbert, B.; Shi, H.; Yeh, J. I.; Zink, J. I.; Nel, A. E. *ACS Nano* **2008**, *2*, 2121−2134.
(21) Elstner, M.; Porezag, D.; Jungnickel, G.; Elsner, J.; Haugk, M.; Frauenheim, T.; Suhai, S.; Seifert, G. *Phys. Rev. B* **1998**, *58*, 7260−7268.
(22) We used the pseudopotentials 030-Zn0gpbe-bm.uspp, 008-O-gpbe-bm.uspp, and 001-H-gpbe-bm.uspp from http://www.physics.rutgers.edu/dhv/uspp/ (accessed October 8, 2012).
(23) Giannozzi, P.; Baroni, S.; Bonini, N.; Calandra, M.; Car, R.; Cavazzoni, C.; Ceresoli, D.; Chiarotti, G. L.; Cococcioni, M.; Dabo, I.; Corso, A. D.; de Gironcoli, S.; Fabris, S.; Fratesi, G.; Gebauer, R.; et al. *J. Phys.: Condens. Matter* **2009**, *21*, 1−19.
(24) CPMD. Copyright IBM Corp. 1990−2004, Copyright MPI fuer Festkoerperforschung Stuttgart 1997−2001.
(25) Köppen, S.; Bronkalla, O.; Langel, W. *J. Phys. Chem. C* **2008**, *112*, 13600−13606.
(26) Aradi, B.; Hourahine, B.; Frauenheim, T. *J. Phys. Chem. A* **2007**, *111*, 5678−5684.
(27) Plimpton, S. *J. Comput. Phys.* **1995**, *117*, 1 −19.
(28) Ohtaki, H.; Radnai, T. *Chem. Rev.* **1993**, *93*, 1157−1204.
(29) Lide, D. R. *Handbook of Chemistry and Physics*; CRC: New York, 2009; pp 5(57)−5(58).
(30) Jorgensen, W. L.; Madura, J. D. *J. Am. Chem. Soc.* **1983**, *105*, 1407−1413.
(31) Horinek, D.; Serr, A.; Geisler, M.; Pirzer, T.; Slotta, U.; Lud, S. Q.; Garrido, J. A.; Scheibel, T.; Hugel, T.; Netz, R. R. *Proc. Natl. Acad. Sci. U.S.A.* **2008**, *105*, 2842−2847.
(32) Cole, M. A.; Voelcker, N. H.; Thissen, H.; Griesser, H. J. *Biomaterials* **2009**, *30*, 1827 −1850.
(33) Monti, S.; Walsh, T. R. *J. Phys. Chem. C* **2011**, *115*, 24238−24246.
(34) Köppen, S.; Langel, W. *Surf. Sci.* **2006**, *600*, 2040 −2050.
(35) Köppen, S.; Langel, W. *Langmuir* **2010**, *26*, 15248−15256.
(36) Schneider, J.; Colombi Ciacchi, L. *J. Am. Chem. Soc.* **2012**, *134*, 2407−2413.
(37) Liu, L.-M.; Zhang, C.; Thornton, G.; Michaelides, A. *Phys. Rev. B* **2010**, *82* (161415), 1−4.
(38) Gaus, M.; Cui, Q.; Elstner, M. *J. Chem. Theory Comput.* **2011**, *7*, 931−948.
(39) Barnard, A. S.; Zapol, P. *Phys. Rev. B* **2004**, *70*, 1−13.
(40) Diebold, U. *Surf. Sci. Rep.* **2003**, *48*, 53 −229.
(41) Skelton, A. A.; Liang, T.; Walsh, T. R. *ACS Appl. Mater. Interfaces* **2009**, *1*, 1482−1491.